Int. J. Heat Mass Transfer. Vol. 21, pp. 1325–1332

0017-9310/78/1001-1325 $02.00/0

VAPORIZATION OF WATER FILMS IN ROTATING RADIAL PIPES*

J. T. DAKIN
Corporate Research and Development Center, General Electric Company, Schenectady, New York 12301, U.S.A.

(*Received* 28 *November* 1977 *and in revised form* 1 *March* 1978)

Abstract—The vaporization of water films in rotating radial pipes is studied experimentally. The data are interpreted with a simple model in which the major unknown quantity is the fraction of the pipe circumference wetted by the film. The vaporization heat-transfer coefficient is expected to be extremely large since the centrifugal acceleration is 10^3–10^4 times larger than the gravitational acceleration which influences the heat transfer to vertical falling films. The data confirm that the heat-transfer coefficient is very large, and provide measurements of the wetted circumference and of the burn-out heat flux. These fall and rise respectively with increasing centrifugal acceleration.

NOMENCLATURE

A, wetted fraction of passage circumference;
g, acceleration due to gravity;
h, heat-transfer coefficient;
k, thermal conductivity;
l, latent heat of vaporization;
L, radial distance from axis of rotation;
P, local static pressure;
q, heat flux;
Q, total heat flow;
R, passage radius;
Re, local film Reynolds number;
$\bar{Re}$, Reynolds number averaged about the passage wetted circumference;
T, temperature;
v, velocity;
W, volumetric water flow rate;
X, exit steam quality;
Z, passage axis coordinate.

Greek symbols

ΔZ, passage length;
ω, angular velocity;
ψ, tilt angle between radial direction and passage axis;
γ, angle describing orientation of tilt with respect to plane of rotation;
θ, azimuthal coordinate in passage;
ρ, density;
ν, kinematic viscosity;
δ, thickness.

Subscripts

m, metal passage wall;
w, water;
s, steam,
z, z direction;
sat, water saturation;
cu, copper;
in, input to passage.

* Work supported in part by the Electric Power Research Institute.

1. INTRODUCTION

THIN water films have a potential new application in cooling the rotating blades of a gas turbine. In a specific design being considered [1], each blade is cooled by a network of near-radial, sub-surface passages. Water travels through each passage as a thin film drawn by the centrifugal force. A mixture of water and steam freely exits the cooling passage at the radial tip of the blade. The steam enters the turbine gas path, and the water is collected in a stationary, annular gutter. In this design the static pressure is nearly constant along the length of the cooling passage, and is equal to the local gas path pressure.

The fluid dynamic and heat-transfer phenomena occurring within the cooling passage are similar to those encountered in annular two-phase flow[2]. For several reasons, however, the empirical relations commonly applied in this field are not applicable to the present problem. First, the liquid film is motivated primarily by the centrifugal body force which, for proposed turbines, is of order 2×10^4 times larger than gravity. The interfacial shear, which plays a crucial role in the stationary two-phase problem, is of little importance here. Second, the two-phase fluid here experiences a Coriolis body force which is of comparable magnitude to the centrifugal since v is of order ωL, and which acts perpendicular to the flow direction. This Coriolis force serves as a phase separator which keeps the liquid film on the wall. The Coriolis force pushes the film to one side of the cooling passage, thereby destroying the axial symmetry common to many stationary systems.

An analytic study of the two-phase phenomena in the radial, rotating cooling passages has been presented elsewhere [3]. The conclusion of that study is that the dominant heat transfer is to the water phase

which travels as a thin, high-velocity film down the cooling passage wall. An estimate of the film heat-transfer coefficient, h_w, may be taken from the work of Dukler [4]* when the usual gravitational acceleration is replaced by the centrifugal acceleration. Due to the large centrifugal acceleration in the turbine, h_w is expected to be large compared to the heat-transfer coefficient associated with the passage wall thermal conductivity. For this reason a precise value of h_w is not required in designing the turbine. The Dukler model may in fact underestimate the true h_w due to the possible influence of rotation-induced instability [5], and of nucleation.

While the turbine design is insensitive to h_w, it is extremely sensitive to the fraction, A, of the cooling passage circumference which the film wets. The number of factors influencing the film circumferential force balance, and hence A, is formidable. The Coriolis force places the film preferentially along the trailing wall of the pipe. Because the Coriolis force is non-conservative, a secondary flow is induced in the film, and viscous forces enter the circumferential force balance. The approximate analysis of Dakin and So [6] treats the circumferential distribution problem for a laminar, fully-developed film having both surface tension and the secondary viscous forces. It is seen there that the Coriolis force may induce "spreading", or a concave film surface. Since the turbine cooling passages follow the contours of the blade surface they may not be exactly radial, and may therefore have small components of centrifugal force acting perpendicular to their axes. The above analysis was extended to the case of near-radial passages by Dakin [7], and closed form solutions to the circumferential distribution problem were obtained. The circumferential problem may be further complicated by turbulence, a circumferential component to the interfacial shear due to Coriolis-induced secondary flow in the steam [3], the developing character of the flow near the passage inlet, and various edge effects [8]. In light of the complexity of the circumferential force balance, A must be determined experimentally.

The purpose of this paper is to report experimental work on rotating two-phase cooling passages similar to those in the proposed gas turbine. In section two a model for the passage heat transfer is presented. The third section deals with experimental methods. The experimental data appear in section four. These results are values of A as a function of various passage parameters, and values of the burn-out heat flux. A discussion of the results appears in Section 5.

2. HEAT-TRANSFER MODEL

The geometric arrangement of the cooling passage is shown in Fig. 1. The passage is a pipe of radius R, and length ΔZ. The center of the pips is located a radial distance L from the axis of rotation, and the pipe orientation is near-radial. Typically $L \gg \Delta Z \gg R$. The

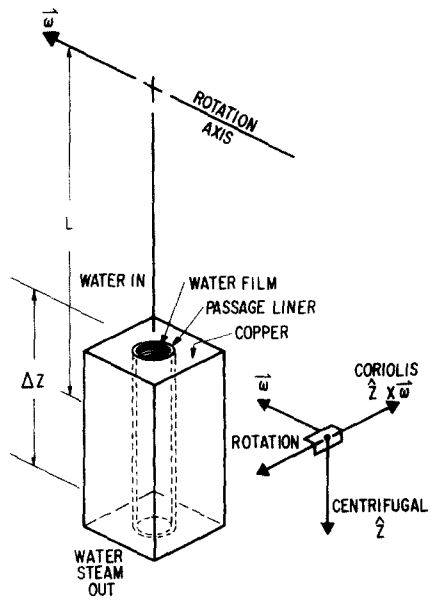

FIG. 1. The construction and orientation of a cooling passage. The directions of the centrifugal and Coriolis forces on the fluid in the rotating reference frame are shown in terms of the vectors $\hat{z}$ and $\vec{\omega}$.

angular velocity is ω. The wall of the passage is lined with an erosion–corrosion resistant liner, most likely a stainless steel, whose effective heat-transfer coefficient is

$$h_m = k_m/\delta_m. \tag{1}$$

The liner is bonded metallurgically to an external copper heat-transfer matrix. Over the range of heat fluxes and water film parameters of interest, the copper matrix is nearly isothermal, and h_m is small compared to h_w.

The inputs to the cooling passage may be expressed as a volumetric water flow rate, W_{in} and a total heat flow, Q_{in}. In the turbine, Q_{in} represents the heat flux entering the airfoil surface integrated over that portion of the surface area serviced by a given cooling passage. In the experiments to be described later, Q_{in} is supplied to the copper by embedded ohmic heaters. Neglecting sensible heating, W_{in} is related to Q_{in} and the latent heat of vaporization of the water

$$W_{in} = \frac{Q_{in}}{X \rho_w l_{ws}}. \tag{2}$$

Here, X represents the exit quality of the two-phase mixture. A turbine design might call for $X = 2/3$, allowing a nominal excess of water as a safety margin. In the experiments, W_{in} will be held constant while Q_{in} and thus X are varied.

The fraction of the passage circumference wetted by the water film is A. While the complex dynamics within the cooling passage dictate that A be determined empirically, it is instructive to consider the results of limited analytic theories. For fully developed laminar

* The Reynolds numbers used by Dukler are four times larger than defined here. See Dukler equation (2).

flow in a radial pipe, A is predicted [7] to be given by

$$A = 0.67\left(\frac{W^2}{\omega^2 LR^5}\right)^{1/7}\left(\frac{W}{Rv_w}\right)^{-1/7}. \quad (3)$$

A crude generalization [3] to the case of turbulent flow, and less restrictive geometries gives

$$A = \text{const.}\left(\frac{W^2}{\omega^2 LR^5}\right)^{0.131}\left(\frac{W}{Rv_w}\right)^{-0.049}. \quad (4)$$

These expressions are seen to show a very weak dependence of A upon the various controlling variables $-v_w$, $\omega^2 L$, and W. The strongest dependence is upon the pipe radius, R.

It will be assumed in the heat-transfer model that A is constant along the (z) length of the cooling passage. This cannot be strictly true both because of the developing character of the flow near the entrance, and because of the decreasing value of W along the length of the passage. It has been shown analytically [3] that the entrance development should occupy a fairly small fraction of the cooling passage length. The above expressions (3)–(4) suggest that the change in A associated with changing W are small. Furthermore, the model will be applied to the data in such a way that a typical, or average A is obtained.

When A is specified, an average film Reynolds number can be written

$$\bar{Re} \equiv \frac{W_{in}}{2\pi RA\, v_w}. \quad (5)$$

This Reynolds number would be everywhere equal to the local film Reynolds number

$$Re \equiv \frac{v_z \delta_w}{v_w} \quad (6)$$

if the local average film velocity, v_z, and the local film thickness, δ_w did not have circumferential and longitudinal variations. Since v_z and δ_w must in reality have such variations, $\bar{Re}$ represents a typical value of Re.

When A is specified and Q_{in} is known, the average heat flux into the water film is readily calculated

$$q = \frac{Q_{in}}{2\pi RA\,\Delta Z}. \quad (7)$$

To extract A from the data, we require *a priori* knowledge of the vaporization heat transfer coefficient. One estimate of this quantity is taken from the model of Dukler [4].

$$h_w = k_w\left(\frac{\omega^2 L}{v_w^2}\right)^{1/3}\left[\left(\frac{1}{3\,Re}\right)^{1/3} + 0.032\,Re^{0.23}\right]. \quad (8)$$

The leading terms are immediately justified on dimensional grounds. The first term in the brackets is the exact laminar theory of Nusselt [9]. The second term in brackets is a fit to Dukler's theory describing the steady transition to turbulent behavior at high Reynolds number. It is assumed that the water has a Prandtl number of unity, and that the interfacial shear is negligible [3].

Dukler's theory and expression [8] give h_w a very weak dependence upon Re in the range $10^2 < Re < 10^4$. There the term in brackets is approximately 0.22. Because of this weak dependence the use of $\bar{Re}$ over the entire wetted circumference and length of the passage is reasonable. It is really $\omega^2 L$, k_w and v_w which determine h_w in this range of Reynolds numbers.

The quantities of prime interest in the turbine design, and the quantities measured in the experiment are Q_{in} and $(T_{cu} - T_{sat})$. These quantities are directly related to A through the expression

$$\frac{Q_{in}}{T_{cu} - T_{sat}} = \frac{2\pi R\Delta ZA}{h_m^{-1} + h_w^{-1}}. \quad (9)$$

Here h_w is related indirectly to A through expressions (5) and (8). Thus equations (5), (8) and (9) constitute a model for the cooling passage in which only one quantity, A, cannot be known *a priori* or measured readily.

As mentioned earlier, the Dukler model will underestimate h_w if nucleation, and/or Coriolis-induced instability are present in the film. For this reason we find it useful to also analyze the data with a deliberate over-estimate of h_w. This is done by assuming h_w to be infinite. As will be seen, the quantities derived from the data are rather insensitive to which assumption is made regarding h_w, especially for large values of $\omega^2 L/g$.

Equation (9) is strictly valid only for infinite copper conductivity and for pure one dimensional conduction. In the actual analysis of the data, a more correct procedure was applied to account for the known copper conductivity and the two dimensional effects on the test specimen.

3. EXPERIMENTAL METHOD

Experiments simulating the conditions of the turbine cooling passages were performed using the motorized test rig shown in Fig. 2. The parameters of the experiment are summarized in Table 1. While other data were taken with other values of some of the parameters, e.g. R, W_{in}, h_m, and P, those data are not reported here.

The test rig consists of a two-armed rotor driven by a variable-speed electric drive train. The rotor rotates in ambient air within a steel enclosure. Cooling water

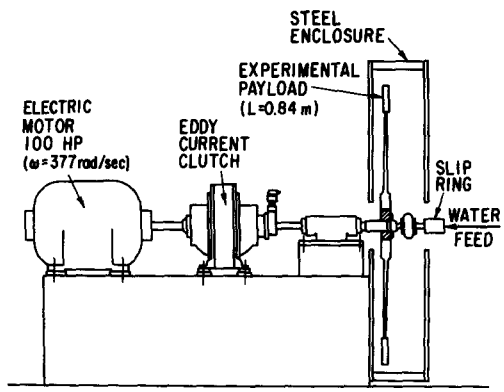

FIG. 2. The motorized test rig.

Table 1. Experimental parameters

L	0.84 m
ω	105, 230, 304, 367 rad s^{-1}
$\omega^2 L/g$	0.9, 4.5, 7.9, 11.5×10^3
ΔZ	0.114 m
R	1.3×10^{-3} m
h_m	5.9×10^4 W m^{-2} C^{-1}
P	1.01×10^5 Pa
T_{sat}	100 C
W_{in}	1.3×10^{-6} m^3 s^{-1}
Q_{in}	0–3000 W

is fed to the rotor through a feed system concentric with the rotation axis. The water is routed to one of the two arms. At the end of that arm is the experimental payload. (A de-activated payload on the other arm balances the rotor.) The water–steam mixture leaving the payload spills freely into the ambient air. Thus the pressure within the payload cooling passage is atmospheric. Electrical heating power and thermocouple signals pass between the rotor and the stationary frame through a silver-graphite slip ring. The effect of dissimilar metals in the thermocouple circuits at the slip rings is minimized by keeping all of these transitions at the same, low, ambient temperature.

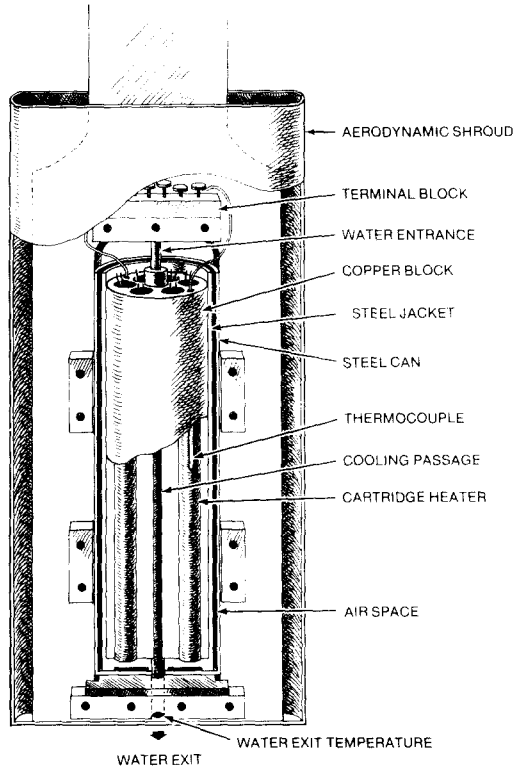

FIG. 3. An experimental payload.

A typical experimental payload is shown in Fig. 3. A copper block is heated by four to six embedded ohmic heaters. A cooling passage runs along the axis of the cylindrical copper block. This passage is lined with a thin-walled stainless steel tube, whose outer surface is metallurgically bonded to the copper. The temperature of the copper block is measured by a redundant set of embedded thermocouples. Significant thermal gradients within the copper are neither expected nor observed. The copper block is encapsulated in a thick-walled stainless steel jacket to limit creep deformation. Air spaces between this jacket, a concentric can, and an outer aerodynamic shroud limit the heat losses to the outside.

The water–steam mixture must travel through 0.02 m of insulation and structural support after leaving the cooling passage but before leaving the arm. A water exit temperature trap device is usually located in this exit path. This device catches some of the exit water for a temperature measurement while allowing the steam to pass freely. Water exit temperature data allows a redundant calorimetry test of measured quantities whenever $T_{cu} < T_{sat}$. Whenever the steam exit quality is finite the water exit temperature gives a measurement of T_{sat}, or alternatively, a test of the thermocouple system.

During some running the water exit temperature is replaced with a direct, radial, unheated exit tube. This allows stroboscopic photography of the water-stream mixture as it leaves the tube.

Two variations on the specimen shown in Fig. 3 are also employed. In one type of specimen the cooling passage is inclined from the radial direction by an angle $\psi = 0.14$ rad. Thus, in this specimen, the centrifugal force has a component directing the fluid to one side of the cooling passage. By rotating this specimen about the radial direction the angle between the off-axis centrifugal force component and the Coriolis force can be changed from $\gamma = 0$ to $\gamma = \pi$.*

The other special specimen has a 1.6×10^{-3} m diameter hole perpendicular to its axis. This hole passes through the steel jacket and the copper, ending at the bond between the copper and the passage liner. There a micro-thermocouple is welded to the outer surface of the passage liner. This thermocouple should read close to T_{cu} if the nearby inner wall of the passage liner is dry and uncooled. If the wall is wet, this thermocouple should read a much lower temperature close to T_{sat}. By rotating this specimen about the radial axis one can crudely determine A.

The normal data recording procedure involves a scan in which ω is fixed, but W_{in} and Q_{in} are varied. Fixed ω is necessary because the ambient temperature and the heat loss from the copper to the ambient vary with ω and with the (unheated) room temperature. The procedure is first to measure the heat loss rate as a function of T_{cu} for the fixed ω and ambient temperature conditions. This is accomplished by turning off the water coolant and turning on the ohmic heaters such that all of the ohmic heat is "lost".

*The angles ψ and γ may be regarded as spherical coordinates describing the local pipe axis orientation. The "polar" angle between the radial direction and the pipe is ψ. The "azimuthal" angle which rotates the pipe about the radial direction with constant ψ is γ. The pipe is in the plane of rotation when γ is 0. The values of ψ and γ vary along the length of a long straight pipe, but are approximately constant here because $\Delta Z \ll L$.

Following the heat loss calibration actual heat-transfer data are recorded. Here W_{in} is held fixed while the ohmic heater power is increased in steps. At each step the copper and water exit temperatures are allowed to stabilize and then recorded. The measured T_{cu} determines the heat loss using the calibration recorded earlier. The difference between the ohmic heater power and the heat loss yields Q_{in}. For Q_{in} values of 1500 W the heat loss represents a 5–10% correction.

The steps in Q_{in} are continued until either the maximum available ohmic power is reached, or a "burnout" occurs. The burnout is distinguished by a rapid rise in T_{cu} accompanying the incremental step in ohmic heater power. The burnout symptoms are similar to what might occur if the coolant water were turned off or completely vapourized. However, neither of these is the case because the water exit temperature device continues to indicate exit coolant in the presence of burnout. Presumably the burnout is a transition to film boiling [3].

4. RESULTS

The results of a typical data scan are shown in Fig. 4. Plotted there is a relation between the heat entering the passage and the copper-saturation temperature difference. The exit steam quality is also shown on the vertical axis. The location of the point $X = 0$ is based on the inlet water temperature, the water flow rate, and the water specific heat. Three distinct heat-transfer

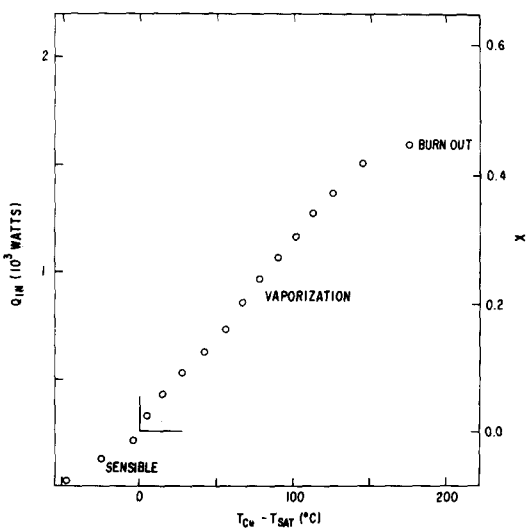

FIG. 4. Data for a radial passage at $\omega^2 L/g = 11.5 \times 10^3$.

regimes are evident. For $X < 0$ there is no net steam generation, and the heat is absorbed as sensible heating of the water. For $X > 0$ steam is generated, and the heat is absorbed primarily in the phase change at temperature T_{sat}. Eventually a third, "burnout" region is reached characterized by falling Q_{in} and rising ($T_{cu} - T_{sat}$). The vaporization region is of prime interest in this paper.

The data from each scan are analyzed to determine

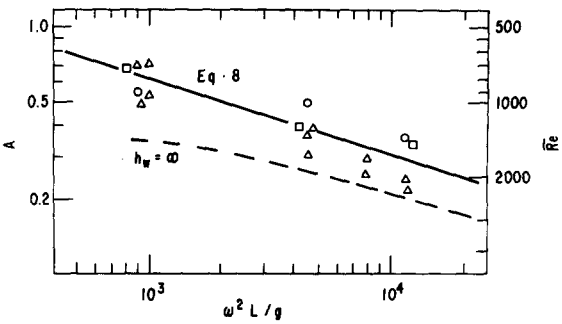

FIG. 5. The observed wetted areas in radial passages. The points are calculated assuming h_w given by equation (8). The different symbols denote different test specimens. The lines are described in the text.

the wetted area, A, and the burnout heat flux, q. These are calculated on the basis of equations (5), (8) and (9), and (7) respectively. The combination of Q_{in} and ($T_{cu} - T_{sat}$) used as input is the highest point on the data scan prior to burnout.

A plot of A vs $\omega^2 L$ appears in Fig. 5. The data are taken from three independent test specimens with radial passages. Each specimen was run at several values of $\omega^2 L$, and the runs were often repeated at later times. The calculated values of A are seen to decline from $A \sim 0.65$ at $\omega^2 L/g = 900$ to $A \sim 0.29$ at $\omega^2 L/g = 11\,500$. The repeated measurements are seen to scatter $\pm 25\%$ about the average value of A. The variations from specimen to specimen are no greater than those from scan to scan with the same specimen.

The trend of the data in Fig. 5 is indicated by the solid line, which has the form $A \propto (\omega^2 L)^{-0.30}$. This fall in A with increasing $\omega^2 L$ is somewhat steeper than expected from equation (4).

The vaporization heat-transfer coefficients used in the calculations are taken from equation (8) and shown in Fig. 6. The metal wall heat-transfer coefficient is also shown in Fig. 6. It is seen that h_w is slightly greater than h_m at the lowest value of $\omega^2 L$, and that it is a factor of three greater at the highest value.

Equation (8) may be viewed as a lower bound on the true vaporization heat-transfer coefficient. In the presence of nucleation and/or rotation induced instability

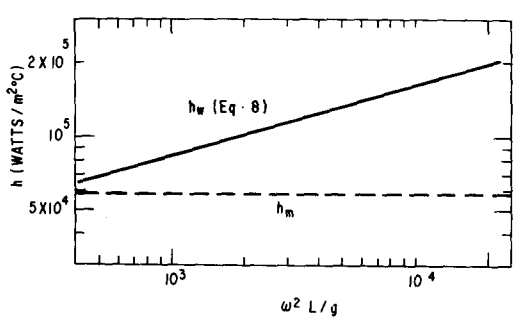

FIG. 6. The vaporization heat-transfer coefficient based on equation (8), and $\bar{R}e \sim 10^3$. The metal wall heat-transfer coefficient is also shown.

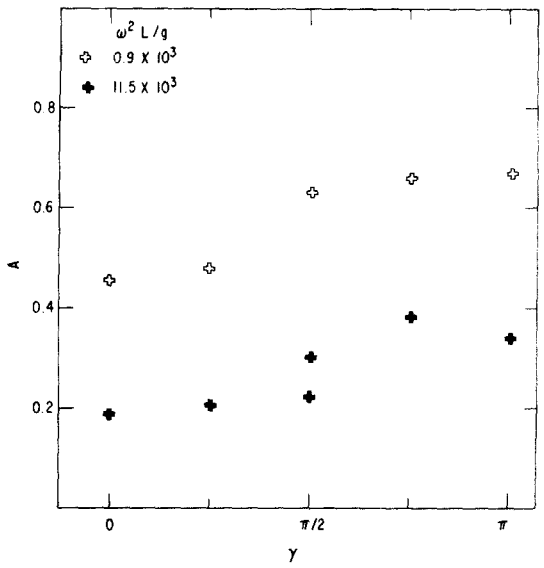

FIG. 7. The variation of calculated A with tilt orientation for a passage tilted by an angle $\psi = 0.14$ rad from the radial direction.

the true heat-transfer coefficient may be higher. In light of this uncertainty in h_w it is instructive to consider the effect of a simple upper bound, $h_w = \infty$. The result of a new analysis on this basis is to shift the trend of the data in Fig. 5 from the solid line mentioned earlier to the dashed line shown below it. The calculated values of A are shifted down a factor of 1.8 at the lowest value of $\omega^2 L$, and down a factor of 1.4 at the highest value. Most likely the "true" values of A lie somewhere between these extremes.

Two test specimens with non-radial passages were also tested. Typical data from one of these specimens are shown in Fig. 7. The values of A shown are calculated assuming that h_w is given by equation (8). The highest values of A are seen to arise when the tilt is oriented such that the Coriolis force is opposed by the off-axis component of the centrifugal force. This occurs when $\gamma = \pi$. The tilted-passage A's show somewhat less scatter than the A's for radial passages, and the trend of increasing A with increasing γ is highly reproducible. The film dynamics model of Dakin [7] shows how an optimum tilt with $\gamma = \pi$ may increase A in a particularly simple laminar flow. It is interesting to note that the range of A's measured in the tilted passage specimens tends to bracker the measurements at corresponding $\omega^2 L$ in the radial passage specimens. This may be seen, for instance, by comparing Fig. 5 to Fig. 7.

The maximum pre-burnout heat fluxes are shown in Fig. 8. The trend of the data is indicated by the straight line, which has the form $q \propto (\omega^2 L)^{0.39}$. The result of a re-analysis assuming $h_w = \infty$ is indicated by the dashed line. At the values of $\omega^2 L/g$ of interest to gas turbine operation ($\sim 2 \times 10^4$) the limiting heat fluxes are greater than 10^7 W/m^2.

It should be noted that in applying these data to a gas turbine design the uncertainty in measured A and measured q due to h_w uncertainty is not significant. This is because the most important quantity in the turbine design is the limit of the product Aq, whose determination does not depend on the assumed value of h_w.

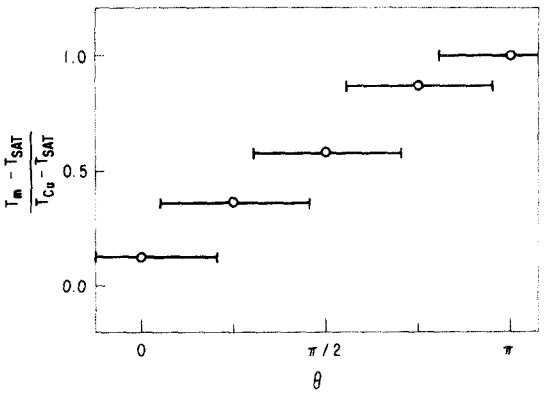

FIG. 9. Temperatures recorded by the micro-thermocouple welded to the outside of a cooling passage liner. These data are recorded with a centrifugal acceleration of $\omega^2 L/g = 11.5 \times 10^3$, and a heat input of $Q_{in} = 1070$ W. The horizontal bars indicate the approximate width of the thermocouple cavity.

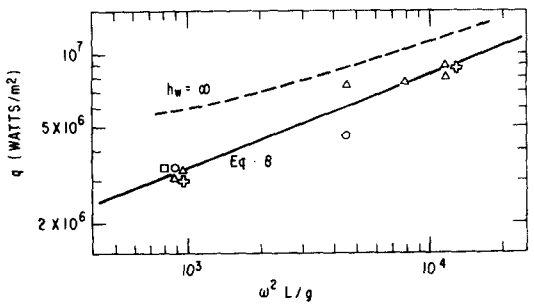

FIG. 8. The maximum pre-burnout heat fluxes. The points are calculated assuming h_w given by equation (8). The different symbols denote different test specimens, and both radial and tilted specimens are included. The lines are described in the text.

Typical data from the micro thermocouple welded to a cooling passage liner are shown in Fig. 9. The thermocouple is located midway along the passage in the z direction, and the thermocouple junction is located in a hole whose width is about 20% of the cooling passage circumference. It is seen that on the side of the passage on which the Coriolis force places the film ($\theta = 0$) the thermocouple registers close to T_{sat}.

On the presumably dry side of the passage ($\theta = \pi$) the thermocouple registers close to T_{cu}. This data crudely but forcefully demonstrates the Coriolis-induced assymetry in the cooling.

A stroboscopic photograph showing the two-phase mixture leaving the end of the arm appears as Fig. 10. There one can clearly see the stratification of the flow into two separate phases. The water flows as a thin,

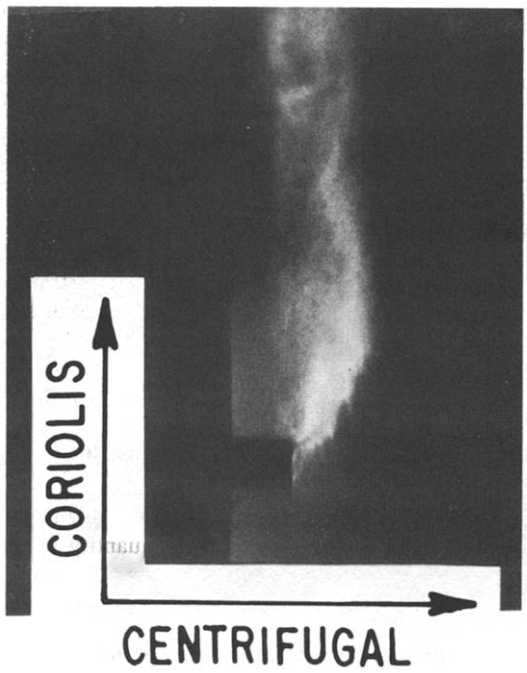

FIG. 10. A stroboscopic photograph showing the water leaving the cooling passage extension. The orientations of the Coriolis and centrifugal forces in the rotating reference frame are shown. The photograph is taken with $\omega^2 L/g = 11.5 \times 10^3$, and $Q_{in} = 0$.

narrow stream along the wall toward which the Coriolis force directs it.

5. DISCUSSION

Heat-transfer data have been accumulated for a rotating, radial cooling passage in which a water film is vaporized. These data have been interpreted in terms of a simple heat-transfer model in which the only unknown parameter is A, the average fraction of the passage circumference wetted by the water film. For a given set of conditions the value of A is determined from the data via the model. The major uncertainty in the model is associated with the water film heat-transfer coefficient, h_w. However, h_w is expected to be sufficiently large that the heat flow to the water is limited not by the water film itself, but rather by the stainless steel wall of the cooling passage.

The measured values of A showed qualitatively the expected response to variations in $\omega^2 L$ and in the passage orientation. Increases in $\omega^2 L$ produced decreases in A. Tilted passages showed increasing A with increasing γ, the angle describing tilt orientation. No attempt was made to provide a correlation relating A to the controlling variables. While a correlation of the form of equation (4) is expected from theoretical considerations, experimental variations in some of the other parameters should be studied before such a correlation is seriously proposed. In addition to the parameters in equation (4), it is possible that quantities such as surface tension and Δz affect A.

At $\omega^2 L/g = 11.5 \times 10^3$, close to the value of interest for a turbine, the behaviour of the cooling system is well determined. The heat-transfer data via the model, the photographic data, and the micro thermocouple data are all consistent with $A = 0.25 \pm 0.05$ for radial passages. The degree of consistency is sufficient to confirm that h_w is at least as high as that given by equation (8). The cooling passage specimens have consistently supported heat fluxes higher than 8×10^6 W/m^2 at this value of $\omega^2 L$ prior to burnout. These heat fluxes are quite adequate for the proposed turbine cooling application.

It is instructive to further consider the implications of the Dukler model for the data in this experiment. We do this for the case of radial pipes, and $\omega^2 L/g = 11.5 \times 10^3$. For these conditions the data in Fig. 5 show $\bar{R}e = 2 \times 10^3$. Turning to Dukler [4], Fig. 3, the film thickness and velocity are readily calculated to be $\delta = 28 \times 10^{-6}$ m and $v = 23$ m/s, respectively, assuming no interfacial shear. This is indeed an extreme example of a thin film. It is sufficiently thin that wall roughness may play a significant role. If nucleation occurs, there is not much opportunity for bubbles to grow before being sheared off, or alternatively, reaching the surface. Several aspects of this film challenge the credibility of any extrapolation from conventional thin film experience.

Acknowledgements—The author wishes to thank Fred Staub, Ralph Wood (GE, CR&D), and Lloyd Trefethen (Tufts University) for discussions concerning aspects of the data. Herman Leibowitz and Ralph Gunst (GE, CR&D) provided crucial contributions to the design, construction and operation of the motorized test rig.

REFERENCES

1. P. H. Kydd and W. H. Day, An ultra high temperature turbine for maximum performance and fuels flexibility, American Society of Mechanical Engineers Paper No. 75-GT-81 (1975).
2. G. F. Hewitt and N. S. Hall Taylor, *Annular Two-Phase Flow*. Pergammon Press, Oxford (1970).
3. J. T. Dakin, Heat transfer in UHT bucket cooling passages, Report No. 77CRD217, General Electric Co. Schenectady (1977).
4. Dukler, Fluid mechanics and heat transfer in vertical falling-film systems, *Chem. Engng Prog. Symp. Ser.* **30**, 1 (1960).
5. Lezius and Johnson, Roll-cell instabilities in rotating laminar and turbulent channel flows, *J. Fluid Mech.* 77, 153 (1976).
6. J. T. Dakin and R. M. C. So, The dynamics of thin liquid films in rotating tubes: approximate analysis, *J. Fluid Engng* **100**, 187 (1978).
7. J. T. Dakin, Viscous liquid films in non-radial rotating tubes, Report No. 77CRD133, General Electric Co., Schenectady (1977).
8. N. Zuber and F. W. Staub, stability of dry patches forming in liquid films flowing over heated surfaces, *Int. J. Heat Mass Transfer* **9**, 897 (1966).
9. W. Nusselt, *Z. Ver. Dt. Ing.* **60**, 541, 569 (1916).

VAPORISATION DE FILMS D'EAU DANS DES TUBES RADIAUX EN ROTATION

Résumé—On étudie expérimentalement la vaporisation de films d'eau dans des tubes radiaux en rotation. Les résultats sont interprétés à l'aide d'un modèle simple dans lequel la principale grandeur inconnue est la fraction de circonférence de tube mouillée par le film. Le transfert thermique par vaporisation est supposé être extrêmement grand puisque l'accélération centrifuge est de 10^3 à 10^4 fois plus grande que l'accélération gravitationnelle qui influence le transfert thermique dans les films tombant verticalment. Les résultats confirment que le coefficient de transfert thermique est très grand et ils fournissent des mesures de la circonférence mouillée et du flux thermique de brûlage. Ceux-ci décroissent et augmentent respectivement lorsque s'accroit l'accélération centrifuge.

VERDAMPFUNG VON WASSERFILMEN IN ROTIERENDEN RADIALEN ROHREN

Zusammenfassung—Die Verdampfung von Wasserfilmen in rotierenden radialen Rohren wird experimentell untersucht. Die Meßwerte werden mit einem einfachen Modell interpretiert, bei dem die Hauptunbekannte der Anteil der durch den Film benetzten Rohrinnenfläche ist. Es wird erwartet, daß der Verdampfungs-Wärmeübergangskoeffizient sehr hoch ist, da die zentrifugale Beschleunigung 10^3 bis 10^4 mal größer als die Erdbeschleunigung ist, welche die Wärmeübertragung an senkrecht fallenden Filmen beeinflußt. Die Meßwerte bestätigen, daß der Wärmeübergangskoeffizient sehr groß ist und liefern Werte für die Benetzung des Umfangs und für den "burnout"-Wärmestrom. Diese verringern und vergrößern sich entsprechend mit wachsender Zentrifugalbeschleunigung.

ИСПАРЕНИЕ ВОДЯНЫХ ПЛЁНОК ВО ВРАЩАЮЩИХСЯ РАДИАЛЬНЫХ ТРУБАХ

Аннотация — Проведено экспериментальное исследование испарения плёнок воды во вращающихся радиальных трубах. Интерпретация полученных данных проводится с помощью простой модели, в которой основной неизвестной величиной является часть окружности трубы, смачиваемая пленкой. Коэффициент теплообмена при испарении имеет очень большую величину в связи с тем, что центробежное ускорение в 10^3–10^4 раз превышает ускорение силы тяжести, что оказывает влияние на перенос тепла к вертикально падающим плёнкам. Экспериментальные данные подтверждают вывод о большой величине коэффициента теплообмена и позволяют определить смачиваемый периметр и критический тепловой поток. Значения последних соответственно уменьшаются и увеличиваются с ростом центробежного ускорения.